Inverse Kinematics of Planar Redundant Manipulators via Virtual Links with Configuration Index

W. J. Chung
Department of Precision and Mechanical Engineering
Chang-Won National University
Chang-Won, Korea

Y. Youm
W. K. Chung*
Department of Mechanical Engineering
Pohang Institute of Science and Technology
P.O. Box 125
Pohang 790-600, Korea

Received September 28, 1991; accepted March 3, 1993

This article presents a new method for generating inverse kinematic solutions for planar manipulators with large redundancy (hyper-redundant manipulators). The proposed method starts by decomposing a planar redundant manipulator into a series of local planar arms that are either 2-link or 3-link manipulator modules, and connecting the conjunction points between them with virtual links. The manipulator then can be handled by a simple virtual link system, which may be conveniently divided into non-singular and singular cases depending on its configuration. When the virtual link system is no longer effective due to a singular configuration, the displacement of the end-effector is then allocated to virtual links according to a displacement distribution criterion. A dexterity index called the "configuration index" distinguishes the non-singular and singular cases. The concept of virtual link is shown by computer simulations to be simple and effective for the inverse kinematics of a planar hyper-redundant manipulator with a discrete model. In particular, it can be applied to solving the inverse kinematics of a SCARA-type spatial redundant manipulator whose redundancy is included in its planar mechanism.

*To whom all correspondence should be addressed.

Journal of Robotic Systems 11(2), 117–128 (1994)

CCC 0741-2223/94/020117-012

この発表では、大きな冗長量を持つプレイナー・マニピュレータ（hyper-redundant マニピュレータ）の転換運動の解を生成する新しい方法について説明する。提案する方法では、最初に、冗長量を持ったプレイナー・マニピュレータを2リンクまたは3リンクのマニピュレータ・モジュールを使いローカル・プレイナー・アームの結合体に分解し、バーチャル・リンクを使ってアーム間の接合点をつなぐ。このように簡単なバーチャル・リンク・システム導入することでマニピュレータの扱いが容易になり、リンク・システムの配置により非特異と特異配置のケースに簡単に分けられる。特異配置のためにバーチャル・リンク・システムが無効になった場合は、エンドエフェクタの変位を、変位分割の規則に従ってバーチャル・リンクに割り当てる。非特異と特異配置のケースは、configuration index と呼ばれる機敏さを表す指標によって特定される。このように、分割モデルを使って大きな冗長量を持ったプレイナー・マニピュレータの転換運動を効果的に簡略化するバーチャル・リンクの概念を、コンピュータのシミュレーションで示す。特に、そのプレイナー・メカニズムの中に冗長量を持つ SCARA タイプのマニピュレータの転換運動の解析に、この方法が適していることを説明する。

1. INTRODUCTION

A kinematically redundant manipulator has more degrees of freedom (dof) than the number of task space coordinates. This redundancy has been used to satisfy many supplementary tasks such as singularity avoidance,[1] obstacle avoidance,[2–3] and keeping the joint variables within their physical limitations,[4,5] by optimizing performance functions such as manipulability measure,[1] condition number,[6] joint range availability,[4,5] manipulator velocity ratio,[7] compatibility index,[8] artificial potential function,[9] and characteristic length.[10] Over the past 2 decades, investigations of redundant manipulators have often been focused explicitly or implicitly on the Jacobian pseudoinverse approach, in which local optimization of performance functions is utilized to resolve redundancy primarily through instantaneous application of the pseudoinverse[11] of the manipulator's Jacobian matrix.

As the need for large redundancy increased, the concept of hyper-redundant manipulators (which have large or infinite degrees of redundancy) was introduced.[12] Implementations of hyper-redundant manipulators can consist of a large number of rigid links that can approximate a continuous morphology,[12] a variable geometry truss,[13] or a flexible physical structure such as a rubber gas actuator device.[14] Applications of hyper-redundant manipulators can include devices for inspection in highly constrained environments,[12,15,16] grasping,[17] and articulated space structures.[14] However, control of these manipulators based on the exact inverse kinematic solutions has been difficult due to the lack of appropriate methods.

An interesting approach to analysis of the kinematics and inverse kinematics of planar continuous and discrete hyper-redundant manipulators was presented by Chirikijan and Burdick.[12] This approach is based on an intrinsic parameterization of a "backbone curve," which captures the macroscopic geometric features of the manipulator, and a modal expansion of the intrinsic curve parameters. In this method, it was assumed that in the discrete structure case the number of links is sufficiently large that the manipulator profile does not substantially deviate from a backbone curve with bounded curvature.

To get the inverse kinematic solutions for the *spatial redundant* manipulators at the *joint position level,* conventional methods such as the extended Jacobian method[18] and the inverse kinematic method[19] require so heavy a burden of computation and symbolic calculation that practical applications are not feasible. Recently, Seraji et al.[20] presented a kinematic analysis of an anthropomorphic 7-dof (degree of freedom) serial link spatial manipulator[21] with a spherical-revolute-spherical (3R-1R-3R) joint arrangement. They parameterized the redundancy by a scalar variable corresponding to the angle between the arm plane and a reference frame. This approach, however, cannot apply to SCARA-type spatial manipulators including planar redundant subarms, although it might be useful for analyzing the kinematics of anthropomorphic arms. A new method is proposed in this article. The planar redundant manipulator is not modeled as a continuous curve, but analyzed by using the "virtual link" concept.[22] For the numerical example, this concept is applied to the inverse kinematics of a SCARA-type spatial redundant manipulator, the Postech-made POSTECH 7-DOF Direct Drive (DD) Robot.[23]

2. VIRTUAL LINK SYSTEM

A virtual link is defined as a fictitious link connecting the conjunction joints between subarms as shown in Figure 1. The virtual link scheme starts by decomposing a planar hyper-redundant arm into multiple subarms consisting of two or three link modules.

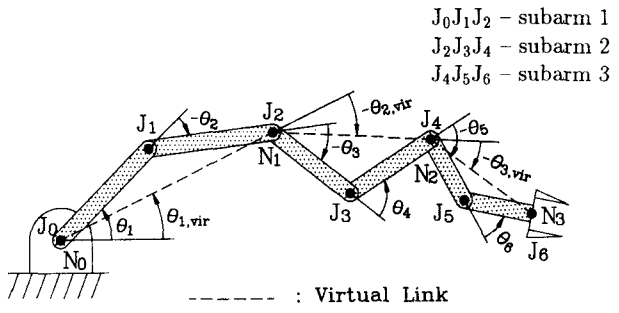

(a)

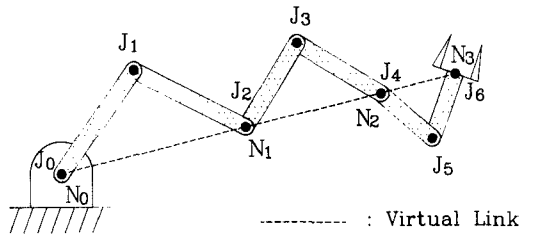

(b)

Figure 1. Virtual link system: (a) non-singular case; (b) singular case.

The constructed virtual link system can experience singular and non-singular configurations as shown in Figure 1. Therefore, the virtual link concept is conveniently divided into the non-singular case and the singular case. For the singular case, a new concept of *displacement distribution scheme* will be added.

2.1. Non-Singular Virtual Link System

In a serially connected planar n-link manipulator, the number n_{vir} of virtual links should be in the range of $n/3 \leq n_{vir} \leq n/2$ because the subarms belong to either two or three link modules. In Figure 1a, three virtual links are shown for a planar 6-dof manipulator. For this manipulator, the conjunction joints N_1 and N_2 are referred to as "nodes," which are connected by virtual links. Whenever the number of virtual links is greater than three, then sub-virtual links will be created until we have subarm modules, defined below. In the case of a planar 10-dof manipulator, as shown in Figure 2, there are four virtual links and two sub-virtual links.

A *subarm module* is defined as the simplest form from which to create a virtual or sub-virtual link, which can be either a two-link or a three-link system.

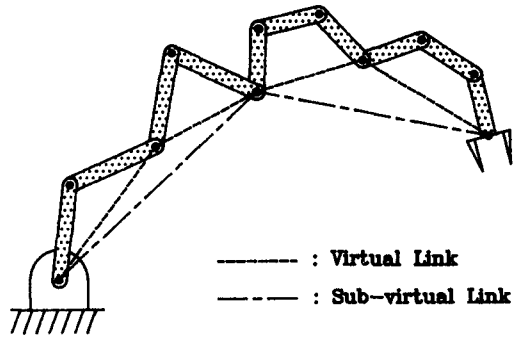

Figure 2. Virtual/sub-virtual link system of the planar 10-dof manipulator.

Such a module is tractable in a virtual link system to solve the inverse kinematic problem for a planar hyper-redundant manipulator. The choice of subarm modules in a virtual link system is based on the following criteria in order of priority, with the results shown in Table I.

Criterion 1: The final goal of a virtual link system should be a form of subarm module with virtual or sub-virtual links.

Criterion 2: A virtual link system should be constructed with as few as possible sub-virtual links. For example, a planar 8-dof manipulator should be a 2-3-3 subarm system rather than a 2-2-2-2 subarm system that, moreover, requires sub-virtual links.

Criterion 3: For a manipulator with less than 10 dof, the number of 3-link modules included in both the subarm system and the virtual link system should be minimized. For example, a planar 6-dof manipulator

Table I. Determination of virtual link systems.

DOF	*Subarm system*	*Virtual link system*	*Sub-virtual link system*
4	2-2	2	0
5	2-3	2	0
6	2-2-2	3	0
7	2-2-3	3	0
8	2-3-3	3	0
9	3-3-3	3	0
10	2-2-3-3	4 (2-2)	2
11	2-3-3-3	4 (2-2)	2
12	3-3-3-3	4 (2-2)	2
13	2-2-3-3-3	5 (2-3)	2
14	2-3-3-3-3	5 (2-3)	2
15	3-3-3-3-3	5 (2-3)	2
16	2-2-3-3-3-3	6 (2-2-2)	3
⋮	⋮	⋮	⋮

should be a 3-link module with a 2-2-2 subarm system rather than a 2-link module with a 3-3 subarm system.

For a task where the orientation of the end-effector is constrained, a 3-link subarm module is preferred to be located near the end-effector.

In solving the inverse kinematic problem of a planar redundant manipulator using the virtual link scheme, first the joint angles of subarm module are calculated. For example, take a planar 6-dof manipulator as shown in Figure 1a. For a given configuration, i.e., $(\theta_1^0, \theta_2^0, \theta_3^0, \theta_4^0, \theta_5^0, \theta_6^0)$, the lengths of virtual links for this manipulator can be determined by

$$\ell_{1,\text{vir}} = \overline{N_0N_1},\ \ell_{2,\text{vir}} = \overline{N_1N_2},\ \ell_{3,\text{vir}} = \overline{N_2N_3}. \quad (1)$$

The joint angles $\theta_{1,\text{vir}}^0$, $\theta_{2,\text{vir}}^0$, and $\theta_{3,\text{vir}}^0$ of the subarm module can be obtained from the inverse kinematics of the 3-link module, which will be discussed in section 3. For the next set point of the end-effector (x_e, y_e), the joint angles $\theta_{1,\text{vir}}$, $\theta_{2,\text{vir}}$, and $\theta_{3,\text{vir}}$ of the virtual link system can be obtained in a similar manner. In turn, the joint angles θ_1, θ_2, θ_3, θ_4, θ_5, θ_6 of the actual manipulator for this set point are computed using the results of joint angles obtained from the subarm module as follows:

$$\theta_1 = \theta_1^0 + (\theta_{1,\text{vir}} - \theta_{1,\text{vir}}^0) \quad (2)$$

$$\theta_2 = \theta_2^0 \quad (3)$$

$$\theta_3 = \theta_3^0 + (\theta_{2,\text{vir}} - \theta_{2,\text{vir}}^0) \quad (4)$$

$$\theta_4 = \theta_4^0 \quad (5)$$

$$\theta_5 = \theta_5^0 + (\theta_{3,\text{vir}} - \theta_{3,\text{vir}}^0) \quad (6)$$

$$\theta_6 = \theta_6^0. \quad (7)$$

Note that the angular displacements of the virtual link system are treated as the displacements *at the nodes*. The other joint angles of the subarms except the joint angles at nodes are unchanged, and the lengths of virtual links are constant as long as the virtual link system works.

When several sub-virtual link systems are nested, the joint angles of the actual manipulator are obtained in the same way mentioned above.

2.2. Singular Virtual Link System

For a short end-effector excursion, the virtual link system is effective as long as it is not in a singular configuration. However, as shown in Figure 1b, a situation might occur where the virtual manipulator cannot move further. A new scheme of the displacement distribution then begins to work. This switching occurs when the configuration index for the virtual link system crosses a threshold value, which indicates a configuration close to a kinematic singularity.

2.2.1. Displacement Distribution Scheme

In this scheme, the lengths of virtual links are changed according to the displacement distribution criterion. The displacement $(\Delta\mathbf{x}_i)$ to be assigned to the i-th subarm is determined by the desired end-effector displacement $(\Delta\mathbf{x})$ multiplied by a displacement distribution weighting factor (w_i), so that

$$\Delta\mathbf{x}_i = w_i\,\Delta\mathbf{x} \quad (8)$$

where $0 \le w_i \le 1$ and $\sum_{i=1}^{s} w_i = 1$; s is the number of subarms. The weighting factor w_i is selected according to the following criterion. Define μ_i for the i-th subarm as:

$$\mu_i \triangleq \begin{cases} |\sin\theta_{i2}| & \text{for a 2-dof subarm} \\ \frac{1}{2}(|\sin\theta_{i2}| + |\sin\theta_{i3}|) & \text{for a 3-dof subarm} \end{cases} \quad (9)$$

where θ_{i2}, θ_{i3} are the second and the third joint angles of the i-th subarm module, respectively. The μ_i provides a simple and efficient way of choosing the displacement distribution weighting factors: simply choose w_i proportional to the μ_i.

It is worth noting that $|\sin\theta_{i2}|$ is just the value of the determinant of the Jacobian matrix of a 2-dof subarm module divided by the product of the two link lengths, which has a physical meaning of manipulability for the subarm. The μ_i for a 3-dof subarm module is the algebraic mean of $|\sin\theta_{i2}|$ and $|\sin\theta_{i3}|$. The objective of this criterion is to assign a large value of the displacement distribution weighting factor to a subarm with high manipulability while excluding the effects of link lengths.

After the end-effector displacement is allocated to the virtual links and then to the subarms, the inverse kinematic problem for the actual manipulator is reduced to that for each subarm module, thanks to the displacement distribution scheme. If that scheme is no longer effective, that is, if the configurations of the subarms are close to singular ones, as shown in Figure 3, the non-singular virtual link system begins to work.

Switching from the non-singular case of the virtual link scheme to the singular case with the dis-

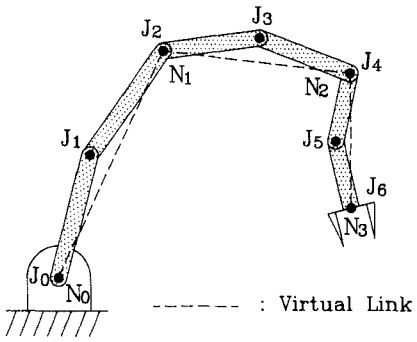

Figure 3. Singular case of the subarm system.

placement distribution scheme is guided by the configuration index. Figure 4 shows a flow chart illustrating the exclusive/complementary use of the two schemes. The proper choice of the threshold value $\text{THRESHOLD}_{\text{vir}}$ (THRESHOLD) for the non-singular virtual link system (subarm system) in this figure is based on the configuration index, which indicates a critical configuration of the virtual link system (subarm system) close to a singularity, such as a fully stretched configuration.

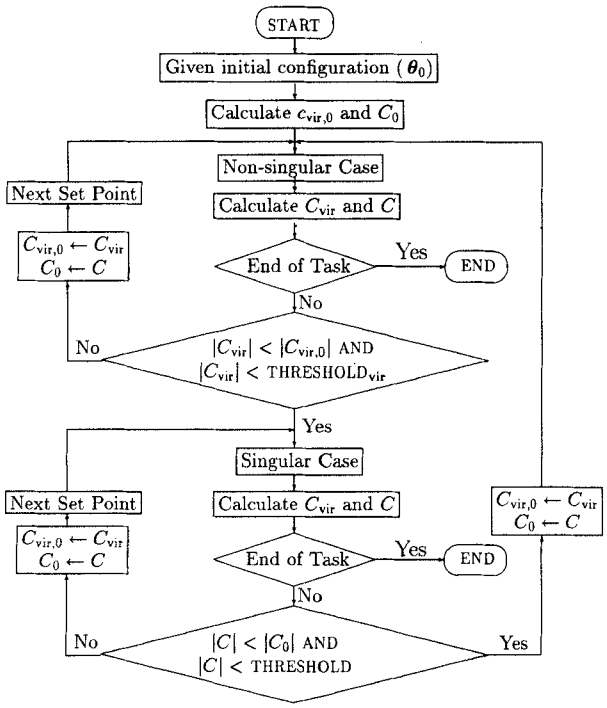

$C_{vir,0}$, C_{vir} : configuration indices for non-singular virtual link system
C_0, C : configuration indices for subarm system

Figure 4. Switching algorithm between the non-singular case and the singular case.

2.3. Configuration Index

For a planar n-dof redundant manipulator decomposed into s subarms, the Jacobian matrix $\mathbf{J} \in \mathcal{R}^{2\times n}$ is given by

$$\mathbf{J} = [\mathbf{J}_1 \vdots \mathbf{J}_2 \vdots \cdots \vdots \mathbf{J}_s] \tag{10}$$

where $\mathbf{J}_1, \mathbf{J}_2, \ldots, \mathbf{J}_s \in \mathcal{R}^{2\times 2}$ (or $\in \mathcal{R}^{2\times 3}$) are the submatrices of $\mathbf{J}$. The configuration index is defined in Chang[19] as:

$$C = \prod_{i=1}^{s} \Delta_i \tag{11}$$

where

$$\Delta_i = \begin{cases} \det(\mathbf{J}_i) & \text{for } \mathbf{J}_i \in \mathcal{R}^{2\times 2} \\ \text{product of minors of rank 2} & \text{for } \mathbf{J}_i \in \mathcal{R}^{2\times 3} \end{cases} \tag{12}$$

As an example, for a planar 8-dof manipulator with a 2-3-3 subarm system the configuration index for the subarm system is given by

$$C = \prod_{i=1}^{3} \Delta_i \tag{13}$$

where Δ_i's for $i = 1, 2, 3$ are

$$\Delta_1 = \det[J^1 J^2] \tag{14}$$

$$\Delta_2 = \det[J^3 J^4] \cdot \det[J^4 J^5] \cdot \det[J^5 J^3] \tag{15}$$

$$\Delta_3 = \det[J^6 J^7] \cdot \det[J^7 J^8] \cdot \det[J^8 J^6]. \tag{16}$$

The J^i in Eqs. (14)–(16) forms the i-th column vector of the Jacobian matrix of the planar 8-dof manipulator. The configuration index for the non-singular virtual link system can be defined similarly. Because the manipulator has a virtual link system in the form of a 3-link module, the configuration index is given by

$$C_{\text{vir}} = \det[J^1_{\text{vir}} J^2_{\text{vir}}] \cdot \det[J^2_{\text{vir}} J^3_{\text{vir}}] \cdot \det[J^3_{\text{vir}} J^1_{\text{vir}}] \tag{17}$$

where J^i_{vir} is the i-th column vector of the Jacobian matrix of the virtual link system.

3. INVERSE KINEMATICS OF 3-LINK MODULES

The inverse kinematic problems of both the virtual link system and the subarm system are ultimately

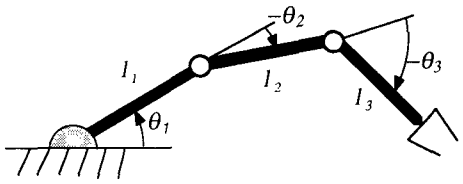

Figure 5. Geometry of the 3-link module.

reduced to those of 2-link and/or 3-link modules. The closed-form solutions for a 2-link module are omitted because they can be derived easily. In this section, the inverse kinematics of 3-link modules is described in detail. The direct kinematic equations for the 3-link arm depicted in Figure 5 are given by

$$\ell_1 \cos\theta_1 + \ell_2 \cos(\theta_1 + \theta_2) + \ell_3 \cos(\theta_1 + \theta_2 + \theta_3) = x \tag{18a}$$

$$\ell_1 \sin\theta_1 + \ell_2 \sin(\theta_1 + \theta_2) + \ell_3 \sin(\theta_1 + \theta_2 + \theta_3) = y. \tag{18b}$$

To get solutions θ_1, θ_2, and θ_3 from a given end-effector position (x, y), an additional equation is required. There are two ways to resolve the redundancy at the inverse kinematic level: (1) a constraint; or (2) optimization of a performance function.

Case 1: Constraint

When a manipulator must do a job such as spray painting or directing a camera to objects, the orientation of an end-effector can be considered as a constraint. Suppose that the end-effector of the arm should be perpendicular to the x-axis in the base frame. This constraint is expressed as

$$\cos(\theta_1 + \theta_2 + \theta_3) = 0. \tag{19}$$

The three nonlinear algebraic equations, eqs. (18a), (18b), and (19), can be solved by a numerical method such as the quasi-Newton method if suitable initial guesses are given.

Case 2: Optimization of a Performance Function

An alternative way to resolve a single redundancy is the extended Jacobian method,[18] which exploits the orthogonality between the gradient vector (∇H) of a performance function ($H(\theta)$) and the null space vector ($\mathbf{n}$) of the manipulator Jacobian matrix of a 3-link module, such as:

$$\boldsymbol{n} \cdot \nabla H = 0. \tag{20}$$

The Jacobian matrix for the 3-link module can be obtained easily, and the null space vector of $\mathbf{J}$ can be obtained as follows:

$$\mathbf{n} = \begin{bmatrix} \ell_2\ell_3 s_3 \\ -(\ell_2\ell_3 s_3 + \ell_1\ell_3 s_{23}) \\ \ell_1\ell_2 s_2 + \ell_1\ell_3 s_{23} \end{bmatrix} \tag{21}$$

where $s_2 \triangleq \sin\theta_2$, $s_3 \triangleq \sin\theta_3$, and $s_{23} \triangleq \sin(\theta_2 + \theta_3)$. A better choice for the performance function $H(\theta)$ is the configuration index, given for a 3-link arm by

$$C = -\ell_2\ell_3 s_3(\ell_2\ell_3 s_3 + \ell_1\ell_3 s_{23})(\ell_1\ell_2 s_2 + \ell_1\ell_3 s_{23}). \tag{22}$$

4. SIMULATION

To demonstrate the effectiveness of the proposed method, planar 7–9-dof manipulators are selected as examples. A planar 8-dof manipulator with revolute joints has 8 links with $\ell_1 = 1.0$, $\ell_2 = 0.8$, $\ell_3 = 0.6$, $\ell_4 = 0.5$, $\ell_5 = 0.4$, $\ell_6 = 0.3$, $\ell_7 = 0.2$, and $\ell_8 = 0.1$ (lengths are given in meters). The given task is to move the end-effector from the initial location $\mathbf{x}_e = [1.5\ 0.0]^T$ to the final location $\mathbf{x}_e = [3.5\ 0.0]^T$ in the positive x-direction with the constant end-effector velocity $\dot{\mathbf{x}}_e = [0.05\ 0.0]^T$ m/s. The initial locations of the first and second nodes are given as (0.5, 0.8) and (1.3, 0.3), respectively (refer to Fig. 6).

The manipulator is given a virtual link system in the form of a 3-link module with a 2-3-3 subarm system. The threshold configuration index values for the virtual link scheme and the displacement distribution scheme are 0.2 and 1.5×10^{-5}, respectively. The first value represents the configuration index for the virtual link system at which the virtual link scheme is replaced by the displacement distribution scheme, while the second value represents the configuration index for the subarm system at which the displacement distribution scheme is replaced by the virtual link scheme. For the displacement distribution scheme, the weighting factors, w_i's for $i = 1$, 2, 3 at each sampling time are 0.80, corresponding to the greatest μ_i; 0.15 for the medium μ_i; and 0.05 for the least μ_i among the three subarms, where the μ_i is given in eq. (9).

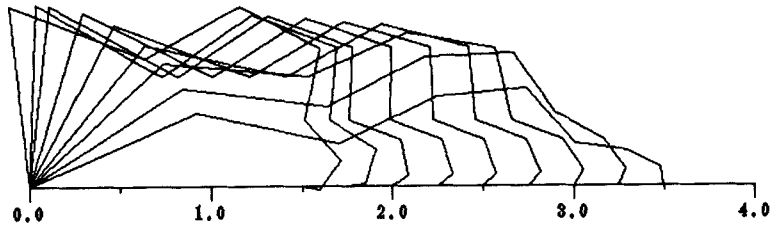

Figure 6. Simulation result of the planar 8-dof manipulator (forward movement).

The 3-link subarm module in the subarm system utilizes the configuration index as a performance function, as does the virtual link system in the form of a 3-link module. Figure 6 illustrates the result of simulation for this planar 8-dof manipulator. As shown in Figure 7, where the manipulability measure given by $\sqrt{\det(\mathbf{J}\,\mathbf{J}^T)}$ is computed using the overall manipulator Jacobian $\mathbf{J}$ for the actual manipulator, the manipulator does not go through any singularity.

Another simulation, for the planar 9-dof manipulator with $\ell_1 = 1.5$, $\ell_2 = 0.8$, $\ell_3 = 0.7$, $\ell_4 = 0.7$, $\ell_5 = 0.4$, $\ell_6 = 0.3$, $\ell_7 = 0.3$, $\ell_8 = 0.2$, and $\ell_9 = 0.1$ with a total length of 5.0 meters, is displayed in Figure 8. This manipulator has a 3-3-3 subarm system and a virtual link system in the form of a 3-link module. For constrained motion of an end-effector, Figure 9 illustrates that the third subarm in a planar 7-dof manipulator that has a virtual link system in the form of a 3-link module is constrained with the end-effector oriented perpendicular to the x-axis.

With respect to computational efficiency, the computational burden of the virtual link method increases on the order of ($n/3 \sim n/2$). However, in existing techniques such as the resolved motion method[4] and the inverse kinematic method[19] it is impossible to obtain the inverse kinematic solutions at the joint velocity/position level, or, at least, extraordinarily complex where possible.

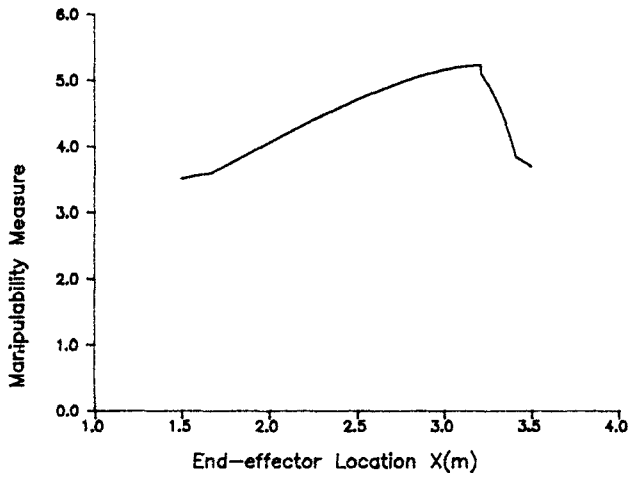

Figure 7. Profile of manipulability measure for the planar 8-dof manipulator.

The above results show that the inverse kinematics of planar redundant manipulators with large redundancy can be obtained easily in a closed form, which has been difficult because of the lack of appropriate methods. The virtual link concept can be applied to SCARA-type spatial manipulators when the redundancy is included in the planar mechanism, as will be discussed in the next section.

5. APPLICATION OF THE VIRTUAL LINK CONCEPT TO A SCARA-TYPE SPATIAL REDUNDANT MANIPULATOR

Although the virtual link concept has many advantages in obtaining exact inverse kinematic solutions for planar redundant manipulators, the generalization of this concept to non-planar manipulators is not simple. However, it can be applied to some special cases. When redundant spatial manipulators have planar serial links, these can be handled by the virtual link concept. To be more specific, when a planar redundant manipulator has a base rotation joint that results in spatial motion, the inverse kinematics of this type of manipulator can be handled easily by the virtual link concept discussed in the previous section. In addition, when a planar redundant manipulator has a spatial 3-dof wrist mechanism, the inverse kinematics of the manipulator can be obtained by separating the wrist mechanism from the planar dof. The simplest case of a base rotation joint with spatial 3-dof wrist mechanism is the POSTECH 7-DOF manipulator. This robot is discussed in this section as an example.

The POSTECH 7-DOF Direct Drive (DD) Robot was designed to have one redundancy including a planar 3-dof subarm. Unlike the simplified model

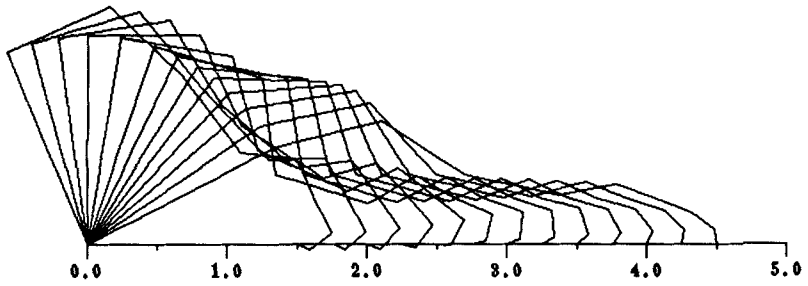

Figure 8. Simulation result of the planar 9-dof manipulator (forward movement).

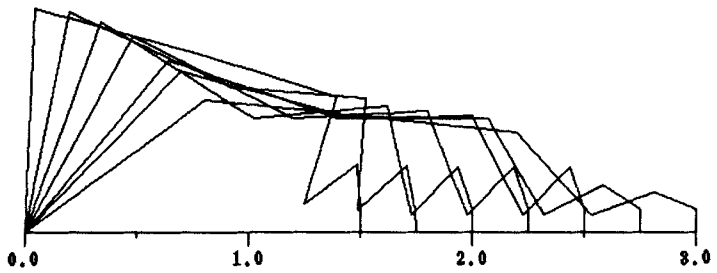

Figure 9. Constraint case of the planar 7-dof manipulator (forward movement).

discussed in the previous sections, a real arm such as that of the POSTECH 7-DOF DD Robot has offset distances between the joints of the planar subarm. The virtual link scheme discussed above must be modified to incorporate this real robot. The overall structure of the robot is shown in Figure 10. The robot is a SCARA-type planar 3R (planar 3-dof)-1R (elbow)-3R (spherical wrist), as shown by the schematics in Figure 11, and has a direct drive mechanism[23] to eliminate mechanical uncertainty and to enable faster motion.

Figure 10. Photograph of POSTECH 7-DOF DD Robot.

5.1. Forward Kinematics

The Denavit-Hartenberg (D-H) link frame assignments are given following the conventional notation. The D-H parameters for the POSTECH 7-DOF DD Robot are shown in Table II. We can obtain the description of the end-effector with respect to the base frame:

$$T = {}^{0}A_1{}^{1}A_2{}^{2}A_3{}^{3}A_4{}^{4}A_5{}^{5}A_6{}^{6}A_7. \tag{23}$$

Table II. D-H parameters for POSTECH 7-DOF DD robot.

i	θ_i	α_i	d_i	a_i
1	θ_1	0°	0	a_1
2	θ_2	0°	d_2	a_2
3	θ_3	90°	$-d_3$	a_3
4	θ_4	−90°	d_4	0
5	θ_5	−90°	$-d_5$	0
6	θ_6	90°	0	0
7	θ_7	180°	$-d_7$	0

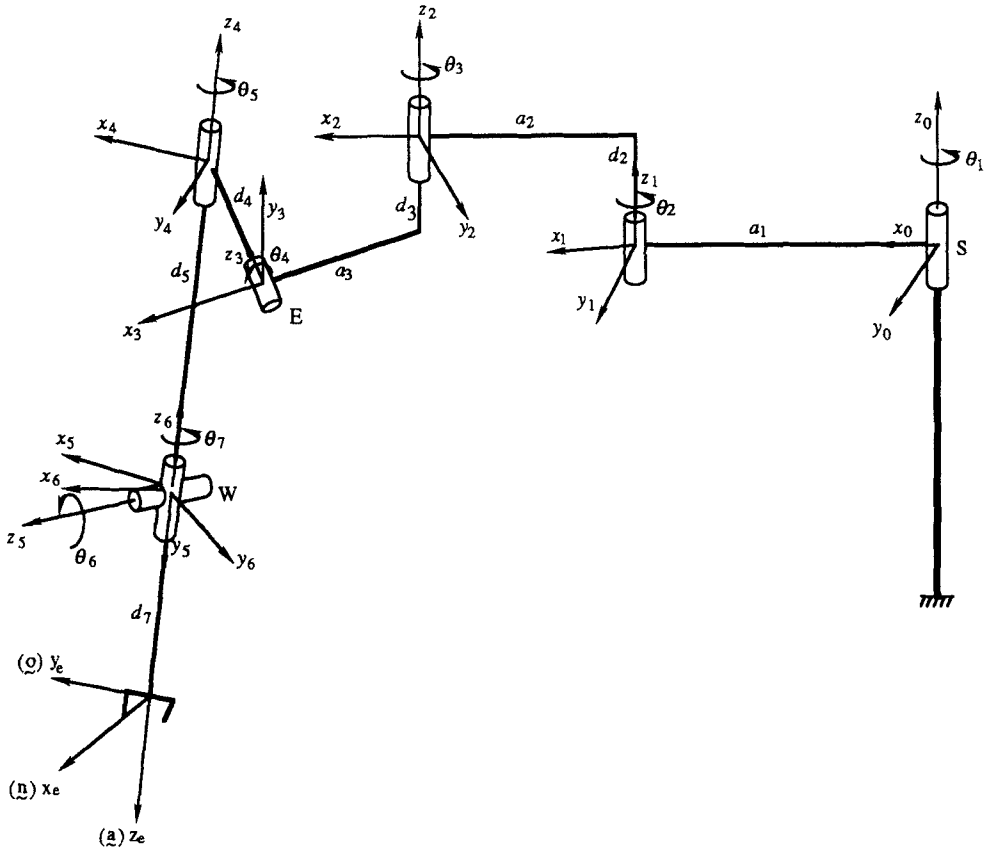

Figure 11. Coordinate system for POSTECH 7-DOF DD Robot.

Hence, the forward kinematics for this robot are completely determined.

5.2. Inverse Kinematics

To separate the inverse kinematic problem of the planar 3-dof subarm from the overall inverse kinematic problem, the position of the wrist and the elbow angle should be determined first in terms of the matrix T.

Wrist Position: Let the given matrix T be specified as:

$$T = \begin{bmatrix} n_x & o_x & a_x & p_x \\ n_y & o_y & a_y & p_y \\ n_z & o_z & a_z & p_z \\ 0 & 0 & 0 & 1 \end{bmatrix}. \tag{24}$$

The left-hand side of eq. (24) can be easily derived in terms of the joint variables $\theta_1, \ldots, \theta_7$. The position of the wrist, (p_x^W, p_y^W, p_z^W), can be obtained from the matrix $T({}^6A_7)^{-1}$ given by

$$T({}^6A_7)^{-1} = \begin{bmatrix} n_xc_7 + o_xs_7 & n_xs_7 - o_xc_7 & -a_x & -a_xd_7 + p_x \\ n_yc_7 + o_ys_7 & n_ys_7 - o_yc_7 & -a_y & -a_yd_7 + p_y \\ n_zc_7 + o_zs_7 & n_zs_7 - o_zc_7 & -a_z & -a_zd_7 + p_z \\ 0 & 0 & 0 & 1 \end{bmatrix}, \tag{25}$$

where $c_7 \triangleq \cos\theta_7$ and $s_7 \triangleq \sin\theta_7$. Hence, p_x^W, p_y^W, and p_z^W are determined as:

$$p_x^W = -a_xd_7 + p_x, \tag{25a}$$

$$p_y^W = -a_yd_7 + p_y, \tag{25b}$$

$$p_z^W = -a_zd_7 + p_z. \tag{25c}$$

Closed-Form Solution of Elbow Angle (θ_4): As shown in Figure 12, the closed-form solution of elbow angle (θ_4) can be determined from the simplified structure

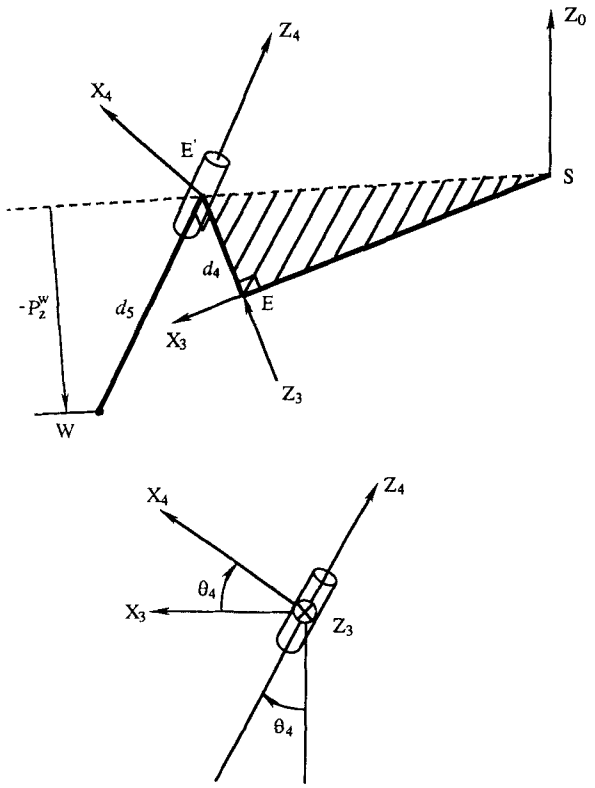

Figure 12. Elbow angle (θ_4).

for the robot, and the following expressions are obtained:

$$c_4 = -\frac{p_z^W}{d_5}, \tag{27}$$

$$s_4 = \pm(1 - c_4^2)^{1/2}, \tag{28}$$

where $c_4 \triangleq \cos\theta_4$ and $s_4 \triangleq \sin\theta_4$. Therefore, the two values of θ_4 are:

$$\theta_{41} = \text{atan } 2(s_4, c_4) \tag{29}$$

or

$$\theta_{42} = \text{atan } 2(-s_4, c_4) = -\theta_{41}. \tag{30}$$

The angles θ_{41} and θ_{42} correspond to ELBOW OUT and ELBOW IN positions of the robot, respectively. The correct value of θ_4 is selected from the above two values by specifying ELBOW OUT and ELBOW IN.

Inverse Kinematics of Planar 3-dof Subarm: The planar 3-dof subarm (ℓ_1-ℓ_2-ℓ_3) is replaced by the virtual link $\ell_{1,\text{vir}}$ as shown in Figure 13. The intermediate variables, $\ell'_{1,\text{vir}}$ and $\theta_{1,\text{vir}}$, are introduced to incorporate the offset distance for further simplification. The relationships among $\ell_{1,\text{vir}}$, $\ell'_{1,\text{vir}}$, $\theta_{1,\text{vir}}$, and $\theta'_{1,\text{vir}}$ are given by

$$\ell_{1,\text{vir}} = \sqrt{(\ell'_{1,\text{vir}})^2 - d_4^2}, \tag{31}$$

$$\theta_{1,\text{vir}} = \theta'_{1,\text{vir}} + \text{atan } 2(d_4, \ell_{1,\text{vir}}). \tag{32}$$

Irrespective of ELBOW OUT and ELBOW IN, $\ell'_{1,\text{vir}}$ and $\theta'_{1,\text{vir}}$ are easily obtained from the geometry shown in Figure 13:

$$\ell'_{1,\text{vir}} = \sqrt{(p_x^W)^2 + (p_y^W)^2} - d_5 s_4, \tag{33}$$

$$\theta'_{1,\text{vir}} = \text{atan } 2(\sin\theta'_{1,\text{vir}}, \cos\theta'_{1,\text{vir}}), \tag{34}$$

where

$$\cos\theta'_{1,\text{vir}} = \frac{p_x^W}{\ell_{1,\text{vir}} + d_5 s_4}, \tag{35}$$

$$\sin\theta'_{1,\text{vir}} = \frac{p_y^W}{\ell_{1,\text{vir}} + d_5 s_4}. \tag{36}$$

Therefore, $\ell_{1,\text{vir}}$ and $\theta_{1,\text{vir}}$ can be obtained from eqs. (31) and (32), and thus the position of the elbow, (p_x^E, p_y^E, p_z^E), is determined as follows:

$$p_x^E = \ell_{1,\text{vir}} \cos\theta_{1,\text{vir}}, \tag{37}$$

$$p_y^E = \ell_{1,\text{vir}} \sin\theta_{1,\text{vir}}, \tag{38}$$

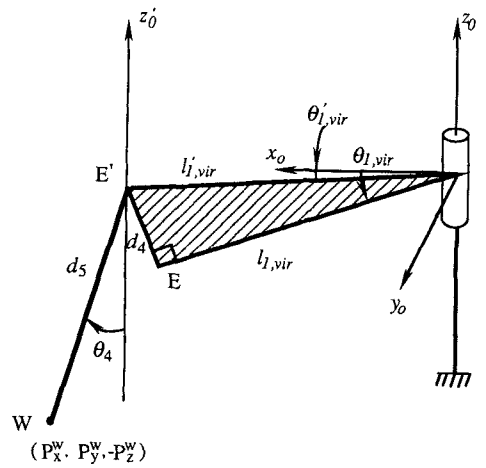

Figure 13. Virtual link for planar 3-dof subarm.

$$p_z^E = 0. \tag{39}$$

Based on the elbow position obtained in the above, we have only to solve the inverse kinematic problem for the planar 3-dof subarm, as discussed in the previous sections. The extended Jacobian method, briefly explained in section 4, is adopted for the inverse kinematics of the planar 3-dof subarm. For known p_x^E and p_y^E, eq. (20) and the kinematic equations given by

$$\ell_1 c_1 + \ell_2 c_{12} + \ell_3 c_{123} = p_x^E \tag{39a}$$

$$\ell_1 s_1 + \ell_2 s_{12} + \ell_3 s_{123} = p_y^E \tag{39b}$$

constitute three non-linear algebraic equations. Hence, the inverse kinematic solutions θ_1, θ_2, and θ_3 at the joint position level can be obtained by solving them. This example illustrates that the virtual link concept can be applied to SCARA-type spatial redundant manipulators although the generalization of the virtual link concept to general spatial robots is difficult.

6. CONCLUSION

This article presented a new method to handle, at the joint position level, the inverse kinematic problem of a discrete planar hyper-redundant manipulator with large redundancy. In the proposed method, the manipulator is not modeled as a continuous curve, but analyzed by using the "virtual link" concept. According to the configuration of the virtual link system, the virtual link system is divided into singular and non-singular cases. For the singular case, the displacement distribution scheme is added. The proposed method simplifies the inverse kinematic problem of a general planar n-dof manipulator to that of a 2-link or 3-link module, which greatly reduces the computational burden. A dexterity index called the configuration index is used to provide a switching criterion between singular and non-singular cases.

As demonstrated by computer simulations, the proposed method was applied effectively to planar 7–9-dof manipulators. In addition to this type of planar manipulator, the virtual link concept was also shown to be applicable to spatial cases such as the planar redundant manipulator with base rotation and spatial wrist joints; POSTECH 7-DOF DD Robot (which has offset distances) was given as an example. These results show that the virtual link concept is effective for obtaining inverse kinematic solutions at the joint position level. The method becomes more useful as the redundant degrees of freedom increase.

REFERENCES

1. T. Yoshikawa, "Analysis and control of robot manipulators with redundancy," in *Robotics Research: The First International Symposium*, M. Brady and R. Paul, Eds., MIT Press, Cambridge, MA, 1984, pp. 439–446.
2. A. A. Maciejewski and C. A. Klein, "Obstacle avoidance for kinematically redundant manipulators in dynamically varying environments," *The International Journal of Robotics Research*, **1**(3), 109–117, 1985.
3. J. Baillieul, "Avoiding obstacles and resolving kinematic redundancy," *Proc. IEEE Int. Conf. on Robotics and Automation*, San Francisco, CA, April 1986, pp. 1698–1704.
4. A. Liègeois, "Automatic supervisory control of configuration and behavior of multibody mechanism," *IEEE Trans. Systems, Man and Cybernetics*, **SMC-7**(2), 868–871, 1977.
5. C. A. Klein and C. H. Huang, "Review of pseudoinverse control for use with kinematically redundant manipulators," *IEEE Trans. Systems, Man and Cybernetics*, **SMC-13**(2), 245–250, 1983.
6. C. A. Klein and B. E. Blaho, "Dexterity measures for the design and control of kinematically redundant manipulators," *The International Journal of Robotics Research*, **6**(2), 72–83, 1987.
7. R. Dubey and J. Y. S. Luh, "Redundant robot control for higher flexibility," *Proc. IEEE Int. Conf. on Robotics and Automation*, Raleigh, NC, April 1987, pp. 1066–1072.
8. S. L. Chiu, "Task compatibility of manipulators posture," *The International Journal of Robotics Research*, **7**(5), 13–21, 1988.
9. O. Khatib and J.-F. Le Maitre, "Dynamic control of manipulators operating in a complex environment," *Proc. 3rd Int. CISM-IFToMM Symp.*, Udine, Italy, 1978, pp. 267–282.
10. J. Angeles, F. Ranjbaran, and R. V. Patel, "On the design of the kinematic structure of seven-axes redundant manipulators for maximum conditioning," *Proc. IEEE Int. Conf. on Robotics and Automation*, Nice, France, May 1992, pp. 494–499.
11. A. Ben-Israel and T. N. E. Greville, *Generalized Inverse: Theory and Applications*, Robert E. Krieger Publishing Co., New York, 1980.
12. G. S. Chirikijan and J. W. Burdick, "An obstacle avoidance algorithm for hyper-redundant manipulators," *Proc. IEEE Int. Conf. on Robotics and Automation*, Cincinnati, OH, May 1990, pp. 625–631.
13. F. Naccarato and P. C. Hughes, *An Inverse Kinematics Algorithm for a Highly Redundant Variable-geometry-truss Manipulator*, JPL Publication 89-45, D. E. Bernad and G. K. Man, Eds., Oxnard, CA, 1989.
14. T. Fukuda, H. Hosokai, and M. Uemura, "Rubber gas actuator driven by hydrogen storage alloy for in-pipe inspection mobile robot with flexible structure," *Proc. IEEE Int. Conf. on Robotics and Automation*, Scottsdale, AZ, May 1989, pp. 1847–1852.

15. H. Kobayashi, E. Shimemura, and K. Suzuki, "A distributed control for hyper redundant manipulator," *Proc. IEEE/RSJ Int. Conf. on Intelligent Robots and Systems*, Raleigh, NC, July 1992, pp. 1958–1963.
16. A. Hayashi and B. Kuipers, "A continuous approach to robot motion planning with many degrees of freedom," *Proc. IEEE/RSJ Int. Conf. on Intelligent Robots and Systems*, Raleigh, NC, July 1992, pp. 1935–1942.
17. G. S. Chirikijan and J. W. Burdick, "Kinematics of hyper-redundant robot locomotion with applications to grasping," *Proc. IEEE Int. Conf. on Robotics and Automation*, Sacramento, CA, April 1991, pp. 720–725.
18. J. Baillieul, "Kinematic programming alternatives for redundant manipulators," *Proc. IEEE Int. Conf. on Robotics and Automation*, St. Louis, MO, March 1985, pp. 722–728.
19. P. H. Chang, "A closed-form solution for inverse kinematics of robot manipulators with redundancy," *IEEE Journal of Robotics and Automation*, **RA-3**(5), 393–403, 1987.
20. K. Kreutz-Delgado, M. Long, and H. Seraji, "Kinematic analysis of 7 DOF anthropomorphic arms," *Proc. IEEE Int. Conf. on Robotics and Automation*, Cincinnati, OH, May 1990, pp. 824–830.
21. J. M. Hollerbach, "Optimum kinematic design for a seven degree of freedom manipulator," *2nd Int. Symposium on Robotics Research*, Kyoto, Japan, August 1984, pp. 215–222.
22. W. J. Chung, W. K. Chung,and Y. Youm, "Inverse kinematics of planar redundant manipulators using virtual link and displacement distribution schemes," *Proc. IEEE Int. Conf. on Robotics and Automation*, Sacramento, CA, April 1991, pp. 926–932.
23. K. W. Jeong, W. K. Chung, and Y. Youm, "Development of POSTECH 7-DOF direct drive robot," in *Robotics and Manufacturing: The Third International Symposium*, M. Jamshidi and M. Saif, Eds., ASME Press, New York, 1990, Vol. 3, pp. 577–582.
24. W. J. Chung, W. K. Chung, and Y. Youm, "Kinematic control of planar redundant manipulators by extended motion distribution scheme," *Robotica*, **10**, 255–262, 1992.